Int. J. Heat Mass Transfer. Vol. 35, No. 2, pp. 383–391, 1992
Printed in Great Britain

0017–9310/92 $5.00 + 0.00

Analysis of the heat transfer coefficient of grooved heat pipe evaporator walls

P. C. STEPHAN and C. A. BUSSE
Joint Research Centre of the Commission of the European Communities,
21020 Ispra (VA), Italy

(*Received* 6 *August* 1990)

Abstract—A model for the radial heat transfer of a grooved heat pipe evaporator is presented. It combines the solution of a two-dimensional heat conduction problem with the calculation of the shape of the liquid–vapour interface and its temperature, taking into account the influence of meniscus curvature and adhesion forces on the volatility of the liquid. It is shown that the common assumption of an interface temperature equal to the saturation temperature of the vapour can lead to a large overprediction of the radial heat transfer coefficient.

INTRODUCTION

HEAT PIPES with open trapezoidal grooves for the liquid transport are of great practical interest as they can easily be fabricated. However, the prediction of the radial heat transfer coefficient of these heat pipes is still a problem.

The radial heat transfer depends on the geometry of the wall and the liquid, and the boundary conditions (see Fig. 1). These are usually the pressure p_v of the vapour inside the heat pipe, which is assumed to be constant over the cross-section, and the temperature T_f at the outside. The symmetry planes between the grooves are adiabatic surfaces. The dry areas of the grooves, where no evaporation occurs, can also be considered as adiabatic if one neglects the relatively small convective cooling of these areas by the vapour. If $\dot{q}_{in}$ is the average heat flux at the outside surface of the heat pipe, the radial heat transfer coefficient is defined by

$$h_{rad} = \frac{\dot{q}_{in}}{T_f - T_{sat}} \tag{1}$$

where T_{sat} is the saturation temperature corresponding to the vapour pressure p_v.

The complications in this two-dimensional heat conduction problem arise from the fact that neither the temperature T_{iv} of the liquid–vapour interface nor its shape are explicitly given.

Several authors [1–5] calculated radial heat transfer coefficients with one- or two-dimensional heat conduction models with the simplifying assumptions that the interface temperature T_{iv} is equal to T_{sat} and that the interface has a constant curvature K. An unknown wetting angle ϑ was incorporated as a free parameter in these models. Both Schneider *et al.* [1] and Shekriladze and Rusishvili [4] derived a correlation for the radial heat transfer coefficient, which describes their numerical results. Comparing the results with experimental data, Schneider *et al.* concluded that the predicted values were too high.

Wayner *et al.* [6, 7] have shown that the assumptions $T_{iv} = T_{sat}$ and $K =$ constant are not valid in a very small 'micro region', where the meniscus comes close to the wall. This is primarily due to the transverse pressure gradient in the liquid phase, which is necessary for transporting the liquid in the micro region to the evaporating surface, and which leads to very large curvatures of the meniscus. These in turn lead to a significant decrease of the volatility of the liquid and a corresponding rise of the interface temperature above T_{sat}. For a correct modelling of these phenomena account must be taken of the interaction between the liquid molecules and the wall atoms in the micro region. The resulting adhesion forces cause a steady transition of the evaporating meniscus into a flat non-evaporating film of microscopic thickness, which is adsorbed on the 'dry' part of the groove. The large curvature of the meniscus in this region creates macroscopically the impression of a finite wetting angle ϑ.

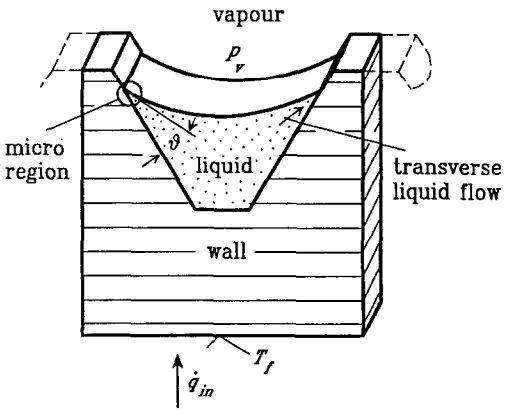

FIG. 1. Element of the heat pipe wall with a liquid filled trapezoidal groove.

NOMENCLATURE

A	dispersion constant [J]
a	top width of the groove [m]
b	bottom width of the groove [m]
f	evaporation coefficient
H	thickness of heat pipe wall [m]
h_{rad}	radial heat transfer coefficient [$W m^{-2} K^{-1}$]
h_{fg}	specific heat of vaporization [$J kg^{-1}$]
K	curvature of the meniscus [m^{-1}]
$\dot{m}$	evaporation rate [$kg m^{-2} s^{-1}$]
n	coordinate normal to the interface [m]
p	pressure [Pa]
Q	heat flow per unit groove length [$W m^{-1}$]
$\dot{q}$	heat flux [$W m^{-2}$]
R	radius of curvature of the meniscus [m]
R_g	gas constant [$J kg^{-1} K^{-1}$]
T	temperature [K]
w	groove width [m]
x	coordinate parallel to the heat pipe wall [m]
y	coordinate normal to the heat pipe wall [m].

Greek symbols

$\delta(\xi)$	shape of the liquid–vapour interface [m]
η	dynamic viscosity [Pa s]
λ	thermal conductivity [$W m^{-1} K^{-1}$]
ν	kinematic viscosity [$m^2 s^{-1}$]
ξ	coordinate parallel to the groove surface [m]
ρ	density [$kg m^{-3}$]
σ	surface tension of the liquid [$N m^{-1}$]
ϑ	apparent wetting angle
φ	half groove angle.

Subscripts

c	capillary
f	outside of the heat pipe wall
in	input
iv	vapour side of the liquid–vapour interface
l	liquid
mac	macro region
mic	micro region
s	solid
sat	saturation
v	vapour
w	groove wall.

Wayner's model was applied by Kamotani to an aluminium/ammonia heat pipe for calculating the heat transfer through the micro region and the apparent wetting angle ϑ [8]. Holm and Goplen combined a simplified version of the Wayner model with a one-dimensional analysis of the radial heat transfer through heat pipe walls with trapezoidal grooves [9].

The objective of the present paper is to analyse quantitatively the consequences which the simplifying assumptions $T_{iv} = T_{sat}$ and K = constant have on the modelling of the radial heat transfer coefficient of a heat pipe evaporator. For this purpose a model has been developed which combines Wayner's treatment of the liquid phase in the micro region with the two-dimensional solution of the heat conduction problem in the cross-sectional area shown in Fig. 1, the 'macro region', which also comprises the micro region.

In the following paragraphs the model equations for the micro and the macro region are presented. The numerical treatment of both regions, their coupling and the iterative computational procedure are explained. Finally, the model is used for computing an example for the radial heat transfer coefficient of the evaporator of an aluminium/ammonia heat pipe. The results are compared with predictions from the simplified models.

† The validity of this assumption we checked by comparing the calculated normal temperature gradients with those parallel to the groove wall, which were found to be several orders of magnitude smaller.

MODELLING OF THE MICRO REGION

The model of the micro region goes back to Wayner *et al.* [6, 7]. We use it in a mathematical form which is similar to that introduced by Kamotani [8].

The heat conduction through the liquid is assumed to be one-dimensional, normal to the wall of the groove.† The extremely small thickness of the liquid layer in the micro region makes it necessary also to consider the interfacial heat resistance. Then the heat flux $\dot{q}$ can be written as

$$\dot{q} = (T_w - T_{iv}) \Big/ \left(\frac{\delta}{\lambda_l} + \frac{T_{sat}\sqrt{(2\pi R_g T_{sat})}}{h_{fg}^2 \rho_v} \frac{(2-f)}{2f} \right) \quad (2)$$

where δ is the local thickness of the liquid layer (see Fig. 2). The temperature T_w of the groove wall in this equation is considered as a function of the ξ-coordinate (Fig. 2) as it depends on the heat conduction through the wall.

The relation between the temperature T_{iv} at the vapour side of the liquid–vapour interface and the saturation temperature T_{sat} is given by

$$T_{iv} = T_{sat}\left(1 + \frac{p_c}{h_{fg}\rho_l}\right). \quad (3)$$

The capillary pressure p_c can be expressed as

$$p_c = \sigma K + \frac{A}{\delta^3}. \quad (4)$$

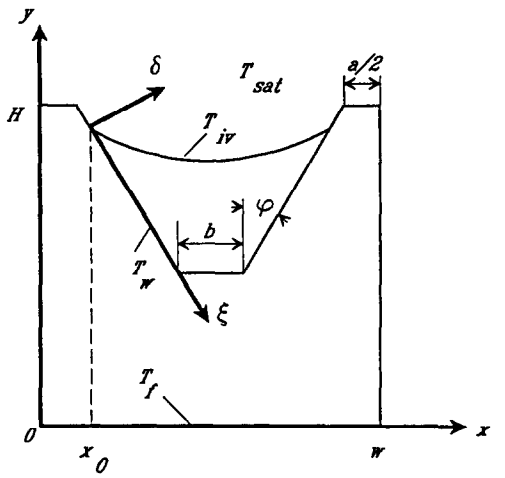

FIG. 2. Coordinate systems, temperatures and groove dimensions.

The first term describes the influence of the meniscus curvature K. The second term is a pseudo capillary pressure which allows one to describe the effect of the adhesion forces. It goes back to the 'disjoining pressure' concept of Deryaguin *et al.* [10]. A is the dispersion constant. Some investigators use the Hamaker constant $\bar{A} = 6\pi A$ instead of A. The curvature K is connected with the thickness of the liquid layer δ by

$$K = \frac{\mathrm{d}^2\delta}{\mathrm{d}\xi^2} \Big/ \left(1 + \left(\frac{\mathrm{d}\delta}{\mathrm{d}\xi}\right)^2\right)^{3/2}. \tag{5}$$

For the modelling of the transverse liquid flow a one-dimensional laminar boundary layer approximation is used in the micro region. From the conservation of mass and the momentum equation the evaporation rate can be expressed as

$$\dot{m} = \frac{\dot{q}}{h_{\mathrm{fg}}} = -\frac{1}{3\nu_{\mathrm{l}}}\frac{\mathrm{d}}{\mathrm{d}\xi}\left(\delta^3\frac{\mathrm{d}p_{\mathrm{c}}}{\mathrm{d}\xi}\right). \tag{6}$$

Combining equations (2) and (6) one obtains a fourth order differential equation for the film thickness $\delta(\xi)$:

$$(T_{\mathrm{w}} - T_{\mathrm{iv}}) \Big/ \left(\frac{\delta}{\lambda_{\mathrm{l}}} + \frac{T_{\mathrm{sat}}\sqrt{(2\pi R_{\mathrm{g}} T_{\mathrm{sat}})}}{h_{\mathrm{fg}}^2 \rho_{\mathrm{v}}}\frac{(2-f)}{2f}\right) = -\frac{h_{\mathrm{fg}}}{3\nu_{\mathrm{l}}}\frac{\mathrm{d}}{\mathrm{d}\xi}\left(\delta^3\frac{\mathrm{d}p_{\mathrm{c}}}{\mathrm{d}\xi}\right). \tag{7}$$

T_{iv} and p_{c} are given as functions of δ by equations (3)–(5). $T_{\mathrm{w}}(\xi)$ has to be provided as an input resulting from the solution of the heat conduction problem in the macro region.

† Rigidly, the temperature at the liquid side of the interface should be used instead of T_{iv}. However, the difference has a negligible influence on the macro heat transfer and the computed T_{w}.

HEAT CONDUCTION MODEL IN THE MACRO REGION

The heat transfer through the heat pipe wall and the liquid in the groove is described by the two-dimensional heat conduction equation

$$\nabla\cdot(\lambda\nabla(T)) = 0 \tag{8}$$

where λ is the thermal conductivity of the liquid or the solid phase, respectively. The boundary conditions are (see Fig. 2):

$T = T_{\mathrm{f}}$ at the outside of the heat pipe wall ($y = 0$),
$\partial T/\partial x = 0$ at the symmetry lines ($x = 0$ and $w/2$),
$T = T_{\mathrm{iv}}$† at the liquid–vapour interface ($x_0 \leqslant x \leqslant w/2$) and
$\partial T/\partial n = 0$ at the 'dry' part of the groove (adsorbed film, $0 \leqslant x \leqslant x_0$), neglecting vapour convection.

NUMERICAL TREATMENT

The calculation of the meniscus shape and heat transfer in the micro region and the solution of the heat conduction problem in the macro region require different numerical approaches. Since the solution of each problem is needed as input for the other one, they are solved in an iterative procedure.

Micro region

The fourth order differential equation (7) is written as a system of four first order differential equations and integrated using a Runge–Kutta method. The unknown wall temperature T_{w} is read from a data file, containing the solution of the macro region.

For the integration the initial values of δ and its first three derivatives have to be specified at $\xi = 0$ where the meniscus is connected to a non-evaporating liquid film. For given temperatures T_{sat} and T_{w}, the capillary pressure p_{c} at $\xi = 0$ follows from $\dot{q} = 0$ with equations (2) and (3). The slope $\mathrm{d}\delta/\mathrm{d}\xi$ is set to zero. K is set to a very small value ($\sigma K \approx 10^{-7} p_{\mathrm{c}}$). The initial value of δ is calculated from equation (4). $\mathrm{d}^3\delta/\mathrm{d}\xi^3$ is chosen so that the integration ends in a meniscus with a desired curvature. The integration is stopped at a value of ξ where the influence of the vapour pressure p_{c} on the interface temperature T_{iv} and the change of the curvature K with ξ have become negligible. Numerical experiments showed that, for given T_{sat} and T_{w}, all menisci in the groove practically do not differ from each other in the micro region. Therefore, it is in general sufficient to compute only a single meniscus in the micro region. The slope of this meniscus then yields the apparent wetting angle ϑ to be used for the calculation in the macro region.

Macro region

Following the work of Schneider *et al.* [1], a finite element method is chosen to solve the heat conduction problem described in equation (8). Triangular elements with quadratic functions are used. As noted by Schneider *et al.*, the mesh generation is most impor-

tant in finding a solution within a desired accuracy. An additional problem is caused by the micro region. The grid width in the micro region is extremely small. On the other hand, the difference in size of two adjacent elements must not be too large to reach convergence. Therefore the numbers of nodes and elements become very high.

The micro region is modelled by several elements. The meniscus curvature outside the micro region is set to a constant value which corresponds to a given capillary pressure outside the micro region $p_{c,mac}$.

The boundary condition at the interface, the temperature T_{iv}, is read from a file containing the solution of the one-dimensional computation in the micro region.

Iteration between micro region and macro region

The iteration procedure is shown in Fig. 3. The calculation is started in the micro region with the given boundary conditions and an assumed constant value of the wall temperature in the micro region $T_{w,mic}$. The computed meniscus shape δ, the apparent wetting angle ϑ, the temperature distribution T_{iv} at the interface and the total heat transferred in the micro region

$$Q_{mic} = \int_{mic} \dot{q}\, d\xi \tag{9}$$

are stored. According to the apparent wetting angle ϑ and the capillary pressure $p_{c,mac}$ the meniscus is then centred in the groove.

The finite element program for the macro region is activated using the interface temperature T_{iv} and the meniscus shape δ calculated before. The resulting heat flux and temperature distribution in the wall and in the liquid are stored.

The computations in the micro and in the macro region are repeated with different constant wall temperatures $T_{w,mic}$, until the computed heat transported through the wall into the micro region has become equal to Q_{mic}.

Now the procedure is started again, using the computed distribution of the wall temperature $T_w(\xi)$ in the micro region instead of a constant value. The iteration is stopped when the results of the two models do not change any more.

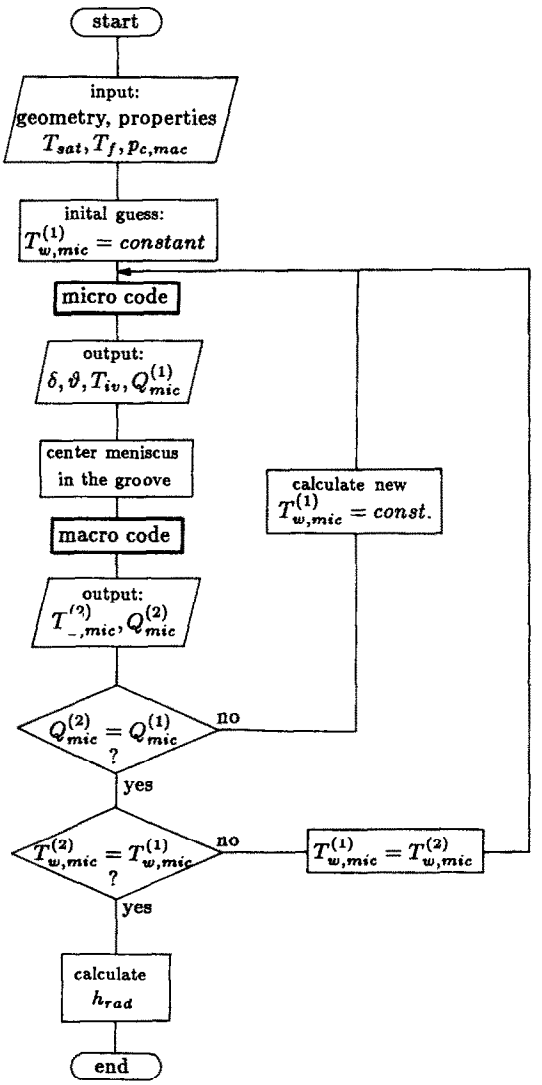

FIG. 3. Iteration scheme for the computation of the radial heat transfer coefficient.

RESULTS AND DISCUSSION

As an example, an aluminium/ammonia heat pipe with $T_{sat} = 300$ K and $T_f = 301.31$ K has been studied. The material properties and the geometry of the groove structure used are listed in Table 1. The grooves were chosen to be of triangular shape.

The value of the dispersion constant A used in the present example has been estimated on the basis of refs. [11, 12], which indicate that these values are usually of the order of 10^{-21} J. However, numerical experiments showed that the dispersion constant has only a small influence on the meniscus shape and on the heat flux. Using a dispersion constant of $A = 1 \times 10^{-21}$ J instead of $A = 2 \times 10^{-21}$ J in the example changed the radial heat transfer coefficient by less than 3%.

The results for the micro region are summarized in Fig. 4, which shows the phenomena occurring in the region where the liquid layer δ is thinner than 10^{-7} m. At first the meniscus approaches the wall with a practically constant slope, which defines the apparent wetting angle ϑ. In this part the meniscus still has essentially the same curvature as in the macro region (the curvature is too small to be noted in the small scale of the diagram). The evaporating heat flux $\dot{q}$ rises in correspondence with the decreasing thickness of the liquid layer. The interface temperature T_{iv} is practically identical to T_{sat} until δ approaches values of 10^{-8} m. Then T_{iv} rises rapidly to the value of the wall temperature T_w at $\xi = 0$, which is 301.0 K. As a result, $\dot{q}$ passes through a sharp maximum of 5300 W cm^{-2} and then drops to zero.

Table 1. Data for the computation of the presented example

Properties of materials (liq.: NH_3; sol.: Al) at $T_{sat} = 300$ K		
Specific heat of evaporation h_{fg}	1180×10^3	J kg^{-1}
Gas constant R_g	488.00	J kg^{-1} K^{-1}
Density of saturated vapour ρ_v	9.00	kg m^{-3}
Density of liquid ρ_l	600.00	kg m^{-3}
Thermal conductivity of solid λ_s	221.00	W m^{-1} K^{-1}
Thermal conductivity of liquid λ_l	0.480	W m^{-1} K^{-1}
Surface tension σ	0.020	N m^{-1}
Dynamic viscosity of liquid η_l	1.30×10^{-4}	Pa s
Dispersion constant A	2.00×10^{-21}	J
Evaporation coefficient f	1.00	—
Groove geometry		
Groove width w	1.0×10^{-3}	m
Groove height H	1.5×10^{-3}	m
Top width a	0	m
Bottom width b	0	m
Half groove angle φ	45.0	deg
Boundary conditions		
Main capillary pressure $p_{c,mac}$	22.0	N m^{-2}
Outer wall temperature T_f	301.31	K

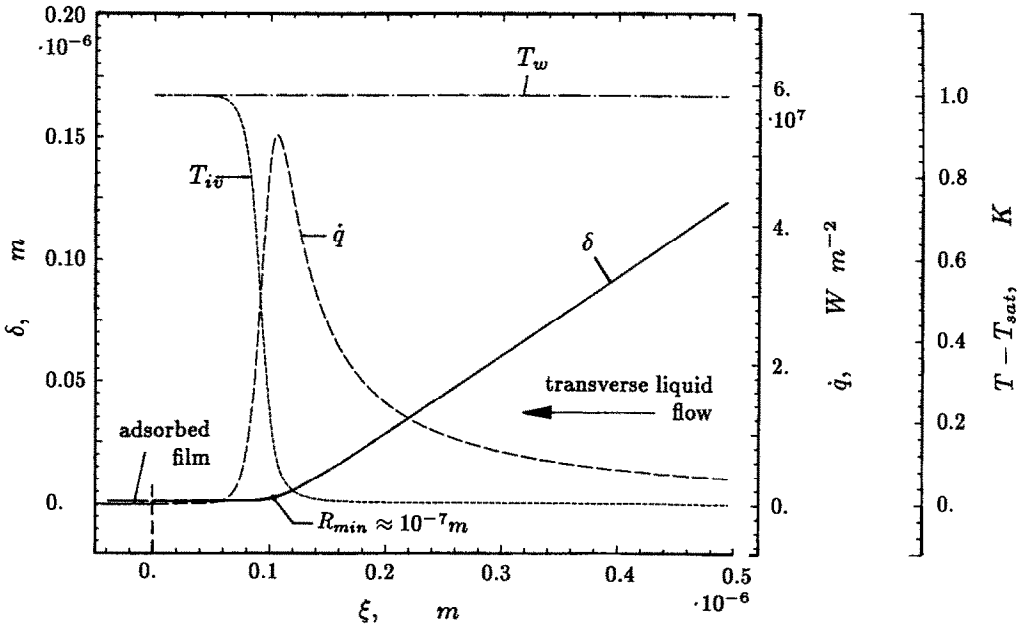

FIG. 4. Meniscus shape, heat flux and interface temperature in the micro region.

The rise in T_{iv} is caused by the increasing capillary pressure p_c (see equation (3)) which is required to drive the transverse flow of the liquid. At the beginning of the rise in T_{iv} the meniscus is still too far away from the wall for the adhesion forces to contribute to p_c, so that the rise in p_c is produced by a strong increase of the curvature of the meniscus ($R_{min} = 1/K_{max} \approx 10^{-7}$ m). This leads to a rapid bending of the meniscus and the generation of a finite apparent wetting angle $\vartheta = 19.7°$. At the end of the rise in T_{iv} the δ^{-3} power of the adhesion force term produces the necessary capillary pressure, while the curvature goes to zero and the meniscus levels off into a flat non-evaporating film.

The total heat transferred per unit groove length in the region up to $\xi = 2 \times 10^{-7}$ m is $Q = 3.4$ W m^{-1}, which agrees with Kamotani's value [8]. The total heat transferred in the micro region (here: $0 \leqslant \xi \leqslant 1 \times 10^{-6}$ m) is $Q_{mic} = 6.6$ W m^{-1}.

The computation in the macro region shows that the transfer of Q_{mic} through the heat pipe wall into the micro region requires an average heat input of $\dot{q}_{in} = 3.0$ W cm^{-2}. The adsorbed liquid film covers about 15% of the groove.

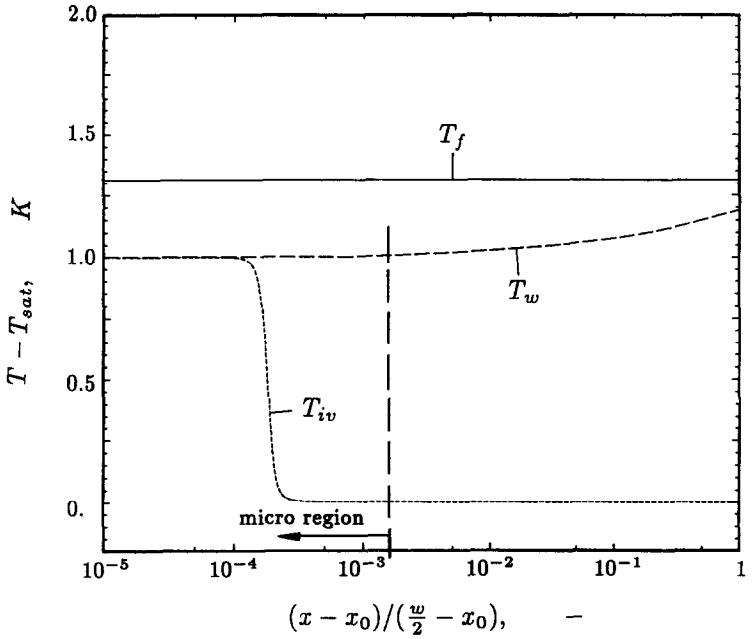

FIG. 5. Plot of T_f, T_w and T_{iv} over a logarithmic, dimensionless length coordinate.

Figure 5 is a semi-logarithmic plot of the temperatures T_f, T_w and T_{iv}. It shows that T_w is nearly constant in the micro region. Therefore it does not seem to be necessary to consider the exact distribution of $T_w(\xi)$ in the micro region. Test calculations have confirmed that the results almost do not change if the correction of the constant wall temperature in the micro region $T_{w,mic}$ is left out (see outer loop in Fig. 3). Figure 6(a) shows the same temperatures over a linear length scale. The rise in T_{iv} appears here as a step change. The radial heat transfer coefficient defined in equation (1) is $h_{rad} = 2.3$ W cm^{-2} K^{-1}. About 23% of the total heat in the groove goes through the very first part of the evaporating film ($0 \leqslant \xi \leqslant 2 \times 10^{-7}$ m) and about 45% through the micro region.

If the interface temperature T_{iv} is set constant to T_{sat}, like in previous papers, a much different temperature distribution appears in the heat pipe wall and in the liquid for the same values of T_f and T_{sat} and the same geometry, as is shown in a comparison of Figs. 6(a) and (b). The top of the groove is now cooled down by evaporation, more heat goes through the evaporator wall ($\dot{q}_{in} = 10.4$ W cm^{-2}) and one gets a higher radial heat transfer coefficient ($h_{rad} = 7.9$ W cm^{-2} K^{-1}). The fraction of heat going through the micro region now is 94%. Figure 7 shows the isotherms in the macro region in the case of a computed interface temperature (Fig. 7(a)) and in the case of a constant interface temperature equal to T_{sat} (Fig. 7(b)). As can be seen, the consideration of the correct interface temperature is decisive for the temperature profile in the whole heat pipe wall, although T_{iv} is different from the saturation temperature only in the micro region. Numerical experiments showed that the distribution of the temperature T_{iv} in the micro region is not so much responsible for the change, but the total temperature rise $T_{iv}(\xi = 0) - T_{sat}$, which governs the temperature of the whole top part of the heat pipe wall.

The essential numerical results are summarized in Table 2. The radial heat transfer coefficient, in the case of a calculation with a constant interface temperature $T_{iv} = T_{sat}$, agrees with the value calculated from the correlation of Schneider within the indicated accuracy of 15% [1]. The present paper shows that this value is about three times too high due to the assumption

Table 2. Essential results of the computation and comparison with simplified models

	Present paper		Schneider [1]	Shekriladze [4]
	$T_{iv} = T(\xi)$	$T_{iv} = T_{sat}$	$T_{iv} = T_{sat}$	$T_{iv} = T_{sat}$
$T_f - T_{sat}$ [K]	1.31	1.31	—	—
$\dot{q}_{in}$ [W cm^{-2}]	3.0	10.4	—	—
Q_{mic}/Q_{in} [%]	45	94	—	—
h_{rad} [W cm^{-2} K^{-1}]	2.3	7.9	~6.9	~3.9

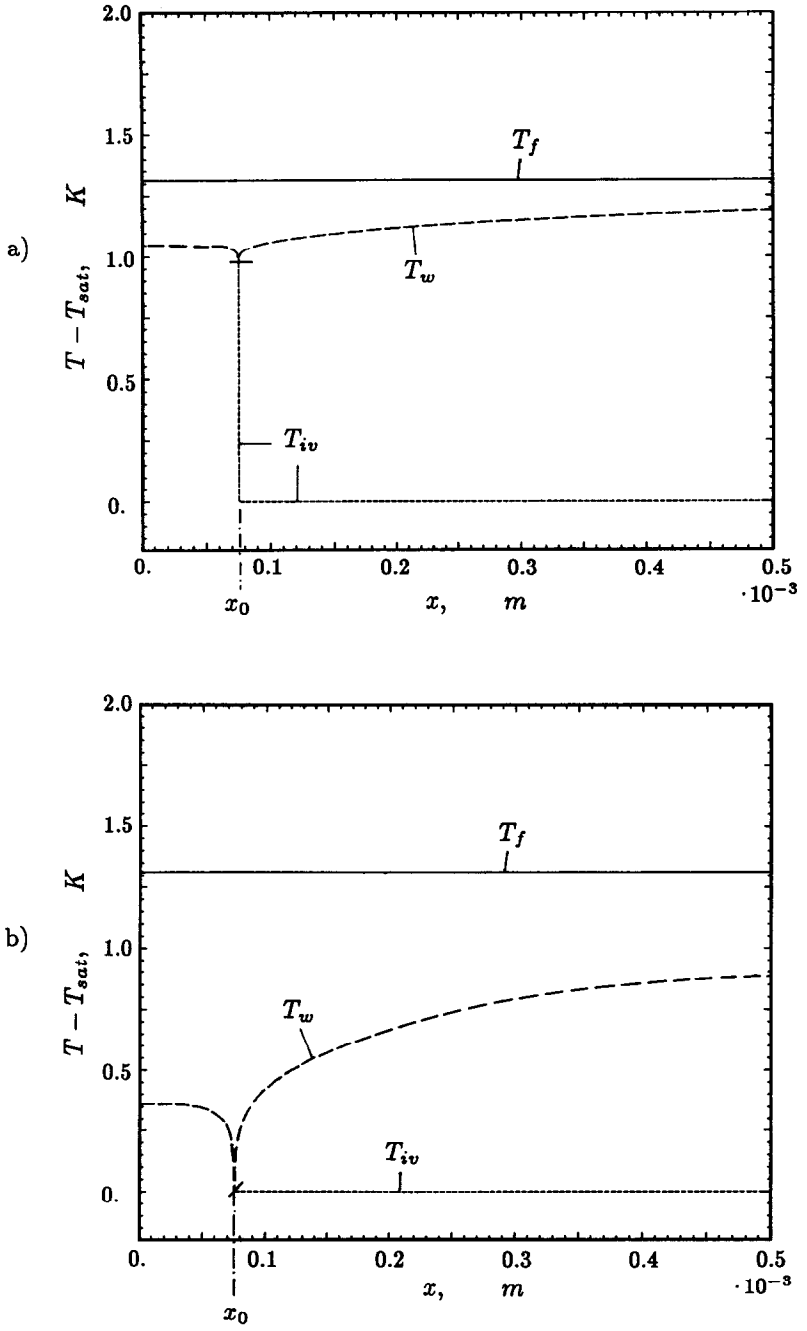

FIG. 6. Computed temperatures in the macro region for given T_f and T_{sat}. (a) Present model. (b) Assuming $T_{iv} = T_{sat}$ and K = constant.

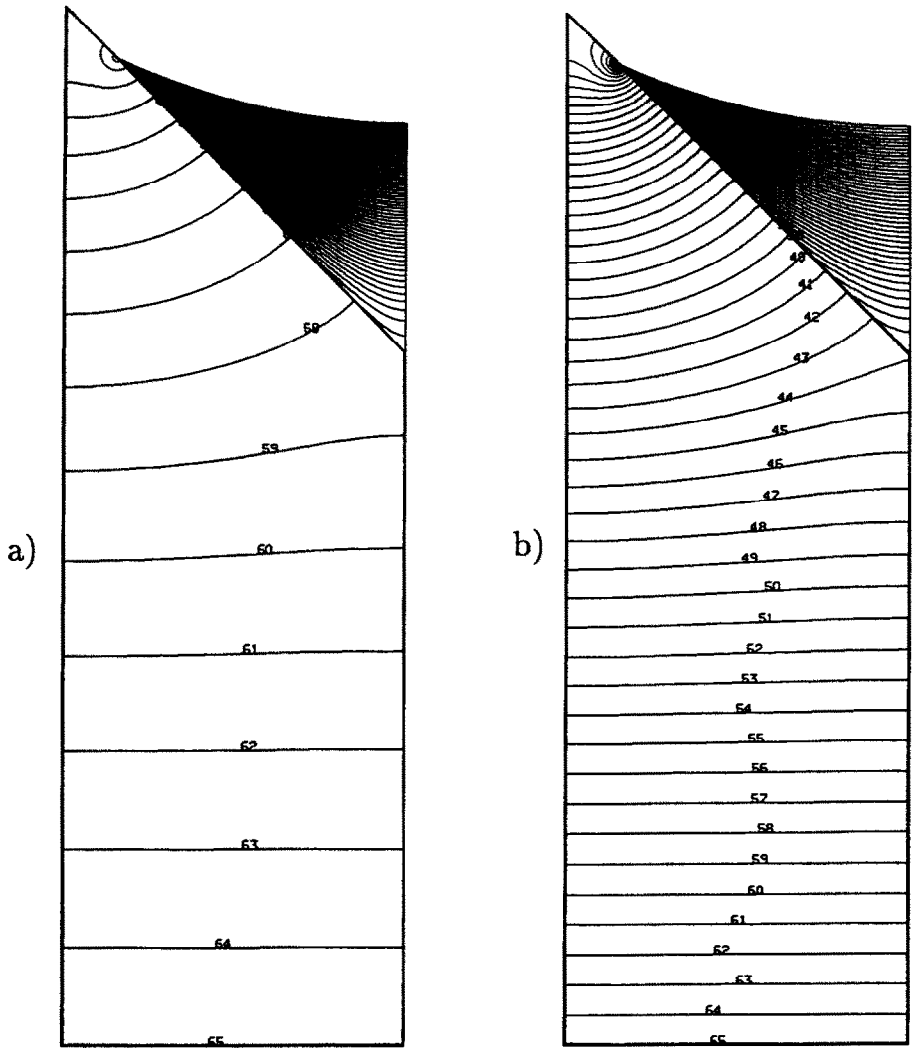

FIG. 7. Isotherms in the heat pipe wall and in the liquid phase. (a) Present model. (b) Assuming $T_{iv} = T_{sat}$ and K = constant (temperature difference between two isotherms: $\Delta T = 0.0202$ K).

of a constant interface temperature. This may explain the difference to the experimental values noted by Schneider. The value calculated with the simplifying correlation given by Shekriladze and Rusishvili [4] is about twice as high as the value in the present paper.

CONCLUSION

The presented model allows the calculation of the radial heat transfer coefficient in heat pipes with open grooves. The given example shows that it is necessary to take into account the influence of meniscus curvature and adhesion forces on the relation between vapour pressure and interface temperature. The micro region where the meniscus comes close to the wall is decisive for the apparent wetting angle and the temperature of the dry part of the groove wall. The assumption of an interface temperature T_{iv} equal to the saturation temperature T_{sat} of the vapour introduces an artificial cooling of the top of the groove and can lead to a large overprediction of the radial heat transfer coefficient.

REFERENCES

1. G. E. Schneider, M. M. Yovanovich and V. A. Wehrle, Thermal analysis of trapezoidal grooved heat pipe evaporator walls, AIAA Paper 76-481 (1976).
2. M. E. Berger and K. T. Feldmann, Analysis of circumferentially grooved heat pipe evaporators, ASME Paper 73-WA/HT-13 (1973).
3. V. J. Sasin and A. A. Borodkin, Analysis of thermal and fluid characteristics of heat pipes with axial grooves, 5th Int. Heat Pipe Conf., Tsukuba (1984).
4. I. G. Shekriladze and D. G. Rusishvili, Evaporation and condensation on grooved capillary surfaces, 6th Int. Heat Pipe Conf., Grenoble (1987).
5. Y. Kamotani, Thermal analysis of axially grooved heat pipes, 2nd Int. Heat Pipe Conf., Bologna (1976).
6. P. C. Wayner, Y. K. Kao and L. V. LaCroix, The interline heat-transfer coefficient of an evaporating wetting film, *Int. J. Heat Mass Transfer* **19**, 487–492 (1976).

7. P. C. Wayner, Adsorption and capillary condensation at the contact line in change of phase heat transfer, *Int. J. Heat Mass Transfer* **25**, 707–713 (1982).
8. Y. Kamotani, Evaporator film coefficients of grooved heat pipes, 3rd Int. Heat Pipe Conf., Palo Alto (1978).
9. F. W. Holm and S. P. Goplen, Heat transfer in the thin-film region, *J. Heat Transfer* **101**, 543–547 (1979).
10. B. V. Deryaguin, S. V. Nerpin and N. V. Churayev, Effect of film transfer upon evaporation of liquids from capillaries, *Bull. Rilem* **29**, 93–97 (1965).
11. N. V. Churayev, Molecular forces in wetting films of polar liquids, *Kolloidnyi Zh.* **36**, 323–327 (1974).
12. J. Gregory, The calculation of Hamaker constants, *Adv. Colloid Interface Sci.* **2**, 369–417 (1969).

ANALYSE DU COEFFICIENT D'ECHANGE DE CHALEUR DE L'EVAPORATEUR D'UN CALODUC A RAINURES

Résumé—On présente un modèle de transfert radial de chaleur à travers l'évaporateur d'un caloduc à rainures. La solution en deux dimensions d'un problème de conduction de la chaleur est couplée à l'estimation de la forme de l'interface liquide–vapeur et sa température. Le modèle prend en compte l'influence de la courbure du ménisque et des forces d'adhésion sur la volatilité du liquide. On montre que l'hypothèse courante, qui suppose l'égalité de la température de l'interface et la température de saturation de la vapeur, peut conduire à une forte surestimation du coefficient d'échange radial de chaleur.

STUDIE DES WÄRMEDURCHGANGSKOEFFIZIENTEN IN DER VERDAMPFUNGSZONE EINES WÄRMEROHRES MIT OFFENEN KAPILLARRILLEN

Zusammenfassung—Ein Modell zum radialen Wärmedurchgang in der Verdampfungszone eines Wärmerohres mit offenen Kapillarrillen wird vorgestellt. Die Lösung eines zweideimensionalen Wärmeleitproblems ist gekoppelt mit der Berechnung der Form und der Temperatur der Grenzkurve zwischen flüssiger und dampfförmiger Phase. Dabei werden sowohl der Einfluß der Krümmung der Phasengrenze, als auch der der Adhäsionskräfte auf die Verdampfung berücksichtigt. Es wird gezeigt, daß die übliche Annahme, die Temperatur der Phasengrenze sei gleich der Sättigungstemperatur des Dampfes, zu einer erheblichen Überschätzung des radialen Wärmedurchgangskoeffizienten führen kann.

АНАЛИЗ КОЭФФИЦИЕНТА ТЕПЛОПЕРЕНОСА ОТ СТЕНОК ИСПАРИТЕЛЯ ТЕПЛОВОЙ ТРУБЫ С НАНЕСЕННЫМИ НА НИХ КАНАВКАМИ

Аннотация—Описывается модель радиального теплопереноса от испарителя тепловой трубы с нанесенными на стенку канавками. Модель включает решение двумерной задачи теплопроводности и определение формы и температуры границы раздела жидкость–пар с учетом влияния кривизны мениска и адгезионных сил на летучесть жидкости. Показано, что общепринятое предположение о равенстве температуры на границе раздела и температуры насыщения нара приводит к значительному завышению коэффициента радиального теплопереноса.